CHIRALITY 25:149–159 (2013)

Synthesis and Characterization of Conformationally Rigid Chiral Pyridine–N-Heterocyclic Carbene-Based Palladacycles with an Unexpected Pd–N Bond Cleavage

KIM HONG NG,[1] YONGXIN LI,[1] WEI XIAN TAN,[1] MINYI CHIANG,[2]* AND SUMOD A. PULLARKAT[1]*

[1]*Division of Chemistry and Biological Chemistry, School of Physical and Mathematical Sciences, Nanyang Technological University, Singapore*
[2]*School of Chemical and Life Sciences, Singapore Polytechnic, Singapore*

ABSTRACT The versatility of a previously developed method for the synthesis of chiral carbene-based palladacycles is demonstrated through the synthesis of two new chiral pyridine-functionalized N-heterocyclic carbene palladacycles with different wingtip groups. The efficiency in their resolution with different counter anions and different chiral amino acid salt auxiliaries has been studied. The absolute stereochemistries of all the chiral compounds were confirmed by single crystal X-ray crystallography. An unexpected Pd–N bond cleavage that resulted in the racemization of the α-carbon center in these complexes has also been investigated. *Chirality 25:149–159, 2013*.

KEY WORDS: N-heterocyclic carbene; palladacycle; conformational study/Pd–N cleavage

INTRODUCTION

The history of carbene complexes can be traced back to 1964, when Fischer successfully characterized the first carbene complex that was coordinated to a tungsten metal center, and approximately 10 years later, Schrock synthesized another class of carbene complexes exhibiting distinctively different characteristics to the Fischer carbene.[1,2] However, it was Arduengo who reported the first crystalline form of a free carbene ligand that fueled the unprecedented development in carbene chemistry in 1991.[3] Compared to phosphines, N-heterocyclic carbenes (NHCs) are mainly strong σ donors and weak π-accepting ligands.[4–9] Due to the strong metal–NHC bond, NHC-based catalytic systems typically exhibit a high degree of stability against heat, moisture, and air during the course of their synthetic applications. Therefore, NHCs have emerged as a popular class of ligands in organometallic catalysis especially in palladium-based catalytic systems.[10–30] Chelating systems are believed to be able to provide a more rigid environment in the course of catalysis, thereby providing more steric control to induce better selectivity in asymmetric scenario.[31] Amino and imino functionalized NHC palladacycles have displayed remarkably enantiomeric excess values of up to 92% in asymmetric allylic alkylation reaction.[32,33] Pyridine-functionalized NHCs have also attracted recent interest and have demonstrated good potential in different catalytic scenarios.[34–46] Crabtree et al.[47,48] and Hahn et al.[49] have previously reported a series of palladium tridentate NHC complexes and successfully applied them to the catalysis of the Heck reaction. A quick literature search revealed that previous efforts in the synthesis of chiral NHC palladacycles typically involved chiral starting materials like (*S*)-(-)-(1,1'-Binaphthalene-2,2'-diyl)bis(diphenylphosphine); BINAP and oxazolines, and to the best of our knowledge, none of the abovementioned pyridine–NHC palladacycles exhibited any chirality in the carbon chelate backbone. We have previously demonstrated an effective method to synthesize chiral pyridine-functionalized NHC palladacycles with a chiral carbon chelate backbone; we hereby extend the efficient and facile synthesis and characterization of a series of pyridine–NHC chelating palladacycles.[50] A thorough conformational analysis of the palladacycles was also undertaken both in solid state and in solution.

RESULTS

The synthesis of palladacycle **1** has been previously reported.[50] The two new palladacycles **2** and **3** were synthesized via a similar methodology starting from the respective imidazolium substrates as shown in Scheme 1. Similar to palladacycle **1**, palladacycles **2** and **3** were insoluble in an array of organic solvents with the exception of dimethyl sulfoxide (DMSO) at 60 °C. Single crystal X-ray crystallography grade crystals of the palladacycles were obtained via slow diffusion of diethyl ether into a MeOH/DMSO solution. The ORTEPs for the newly synthesized palladacycles are shown in Figures 1 and 2. Racemic palladacycles **2** and **3** were crystallized in a centrosymmetric space group. This study revealed that the six-membered chelate rings of the palladacycles are in the boat confirmation, with the phenyl group on the sp^3 carbon of the ring occupying the axial position. The selected bond lengths and angles are given in Tables 1, 2, and 3. Both palladacycles **2** and **3** do not exhibit any marked differences in terms of bond lengths and angles as compared to their analog **1**. The single X-ray crystallography-based analysis of palladacycle **2** further revealed that Cl(2) being *trans* to the NHC will experience a stronger *trans* effect as compared to Cl(1) which is *trans* to a N atom. The *trans* effect is evident in the elongation of 0.062 Å in the Pd(1)–Cl(2) bond compared to the Pd(1)–Cl(1) bond.

Additional Supporting Information may be found in the online version of this article.

Contract grant sponsor: We thank Nanyang Technological University for support of this research (MOE2009-T2-2-065) and for a research scholarship to MC..

*Correspondence to: Sumod A. Pullarkat, Division of Chemistry and Biological Chemistry, School of Physical and Mathematical Sciences, Nanyang Technological University, Singapore 637371. E-mail: sumod@ntu.edu.sg; Minyi Chiang, School of Chemical and Life Sciences, Singapore Polytechnic, Singapore. E-mail: chiang_minyi@sp.edu.sg

Received for publication 28 May 2012; Accepted 09 August 2012
DOI: 10.1002/chir.22116
Published online 18 January 2013 in Wiley Online Library (wileyonlinelibrary.com).

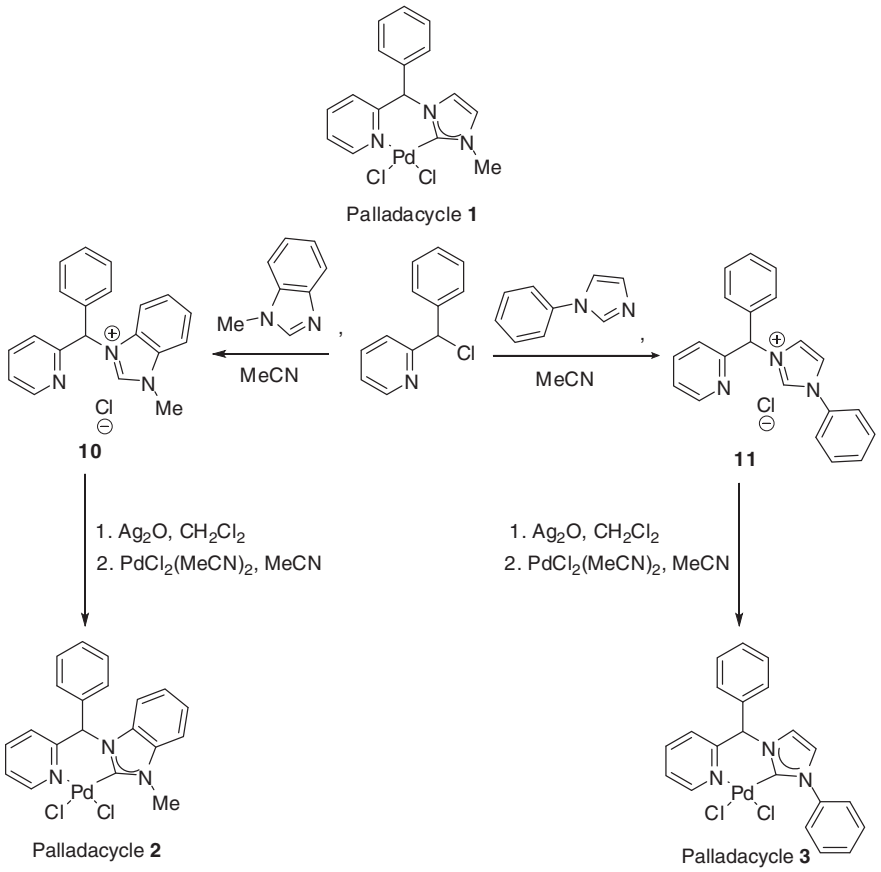

Scheme 1. Synthesis of pyridine–NHC palladacycles **2** and **3**.

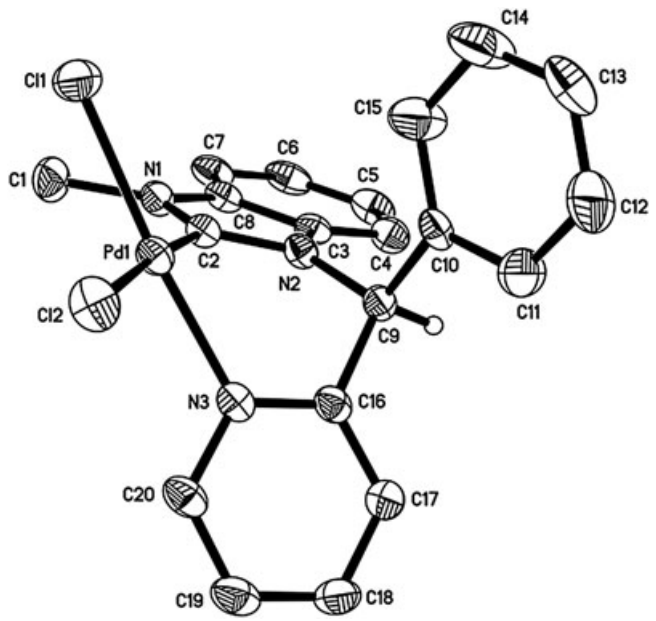

Fig. 1. ORTEP representation of palladacycle **2** (50% probability ellipsoids shown with selected hydrogen atoms omitted for clarity).

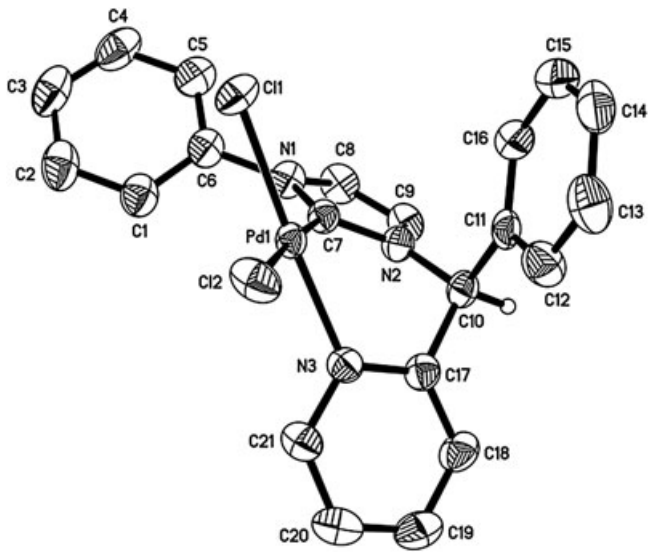

Fig. 2. ORTEP representation of palladacycle **3** (50% probability ellipsoids shown with selected hydrogen atoms omitted for clarity).

The palladium center is in a square planar geometry with a small tetrahedral distortion angle of 2.55° between the {N(3)–Pd(1)–C(2)} and {Cl(1)–Pd(1)–Cl(2)} planes. The NMe group in the carbene moiety and that of the six-membered CN chelate are projecting towards the opposite sides of the square plane. Likewise, for palladacycle **3**, the *trans* effect is evident in the elongation of 0.068 Å in the Pd(1)–Cl(2) bond when compared to the Pd(1)–Cl(1) bond. The palladium

TABLE 1. Selected bond lengths (Å) and angles (º) for palladacycle 2

Pd(1)–C(2)	1.952(3)	Pd(1)–N(3)	2.051(2)
Pd(1)–Cl(1)	2.307(8)	Pd(1)–Cl(2)	2.369(7)
C(2)–N(1)	1.343(3)	C(2)–N(2)	1.351(3)
C(8)–N(1)	1.394(3)	C(3)–N(2)	1.394(3)
C(1)–N(1)	1.463(4)	C(9)–N(2)	1.471(3)
C(2)–Pd(1)–N(3)	85.53(10)	C(2)–Pd(1)–Cl(1)	91.01(8)
N(3)–Pd(1)–Cl(1)	174.71(6)	C(2)–Pd(1)–Cl(2)	175.88(8)
N(3)–Pd(1)–Cl(2)	90.36(6)	Cl(2)–Pd(1)–Cl(1)	93.07(3)
N(1)–C(2)–Pd(1)	133.7(2)	N(2)–C(2)–Pd(1)	119.14(19)
C(16)–N(3)–Pd(1)	121.09(18)	C(20)–N(3)–Pd(1)	118.84(19)

TABLE 2. Selected bond lengths (Å) and angles (º) for palladacycle 3

Pd(1)–C(7)	1.963(3)	Pd(1)–N(3)	2.052(2)
Pd(1)–Cl(1)	2.287(8)	Pd(1)–Cl(2)	2.355(8)
C(7)–N(2)	1.350(3)	C(7)–N(1)	1.347(4)
C(9)–N(2)	1.371(4)	C(8)–N(1)	1.396(4)
C(10)–N(2)	1.471(4)	C(6)–N(1)	1.438(4)
C(7)–Pd(1)–N(3)	86.06(10)	C(7)–Pd(1)–Cl(1)	91.81(8)
N(3)–Pd(1)–Cl(1)	176.64(7)	C(7)–Pd(1)–Cl(2)	176.05(9)
N(3)–Pd(1)–Cl(2)	90.78(7)	Cl(2)–Pd(1)–Cl(1)	91.24(3)
N(1)–C(7)–Pd(1)	136.1(2)	N(2)–C(7)–Pd(1)	119.0(2)
C(17)–N(3)–Pd(1)	121.12(19)	C(21)–N(3)–Pd(1)	120.3(2)

TABLE 3. Comparison of selected bond lengths (Å) and angles (º)

Palladacycle	**1**	**2**	**3**
Carbene C–Pd/Å	1.951(3)	1.952(3)	1.963(3)
Pd–Cl bond elongation/Å	0.064	0.062	0.068
Carbene carbon–Pd–Cl/°	90.8(7)	91.01(8)	91.81(8)

center is in a square planar geometry with minimal tetrahedral distortion angle of 0.16° between the {N(3)–Pd(1)–C(7)} and {Cl(1)–Pd(1)–Cl(2)} planes. Similar to palladacycle **2**, the NPh group in the carbene moiety and the CN chelate palladacycle **3** is also projecting in the opposite side of the square planar palladium center. Due to the bulkiness of the Ph group in palladacycle **3**, the NPh group is tilted at 42.8° away from the plane of the imidazole ring to avoid any unfavorable steric interaction with the Cl(1).

In the context of potential application of these complexes in asymmetric catalysis scenarios, it is imperative to confirm whether the axial orientation adopted by the phenyl group was indeed retained in solution. The conformation of palladacycle **2** in solution was thus determined by two-dimensional (2D) Proton–proton rotating-frame Overhauser effect spectroscopy nuclear magnetic resonance (^{1}H–^{1}H ROESY NMR) analysis (Fig. 3). The assignment of proton signals was made by a combination of correlation spectroscopy, heteronuclear multiple quantum coherence, and heteronuclear multiple-bond correlation. Figure 1 shows the numbering scheme of the protons with the protons numbered in accordance to their respective carbons. From the key correlation (A) seen in the ROESY NMR, there is a strong interaction between H9–H17 and H9–H4. Therefore, the presence of the palladacycle **2** in the boat conformation in solution with the phenyl ring in the axial position can be established. In addition, as illustrated in Figure 4, if the other isomer with the Ph group in the equatorial position is indeed present in the solution, correlations between the H11–H15 protons with both the H17 and H4 protons should be observable in the 2D ^{1}H–^{1}H ROESY NMR spectrum. However, these correlations were conspicuously absent. Therefore, it can be concluded that in solution, no rotational conformers were present (at least in significant amounts so as to be detected by the ROESY experiment), and palladacycle 2 remained locked as it was in solid state in the boat conformation with its Ph group in the axial position. Similarly, the conformation of palladacycle **3** in solution was also determined by 2D ^{1}H–^{1}H ROESY NMR (Fig. 5). Figure 2 shows the numbering scheme of the protons, with the protons numbered in accordance to their respective carbons. The key correlation (A) shows that a strong interaction is present between the H10 and H18 and H10 and H9 protons. This indicated that palladacycle **3** is in a boat conformation with the phenyl group in the axial position.

As shown in Figure 6, if palladacycle **3** is able to undergo ring flipping, the presence of the other rotational conformer with the α-phenyl group in the equatorial position should be

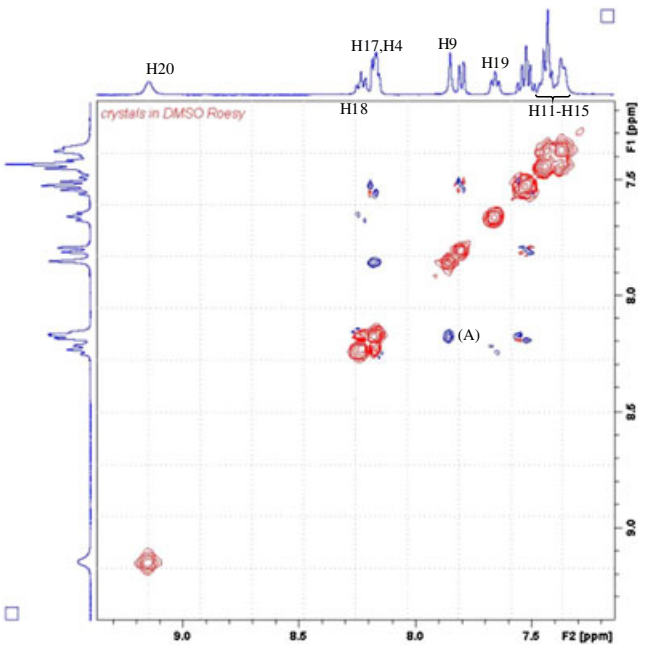

Fig. 3. 2D ^{1}H–^{1}H ROESY NMR of palladacycle **2**.

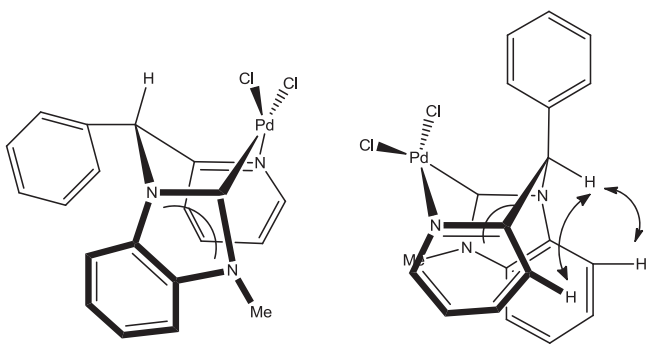

Fig. 4. Two possible ring conformations for palladacycle **2**.

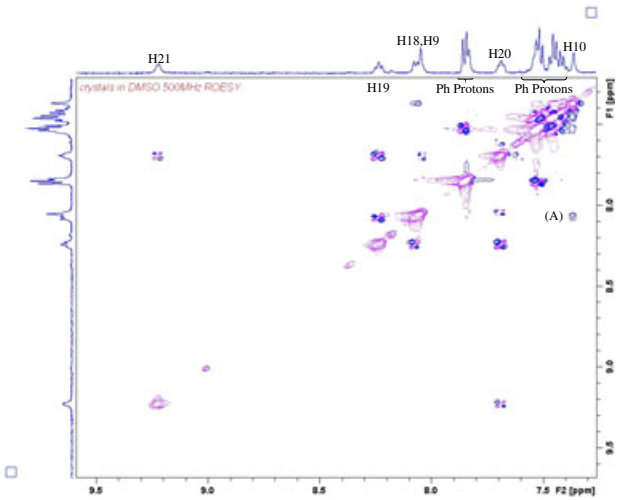

Fig. 5. 2D ^{1}H–^{1}H ROESY NMR of palladacycle **3**.

detected in the 2D ^{1}H–^{1}H ROESY NMR spectrum. Although in this instance, the correlation signals of H12–H16 cannot be assigned conclusively due to overlapping with the H1–H5 protons; however, from the absence of any correlations between the Ph protons with both H18 and H9 in the 2D ^{1}H–^{1}H ROESY NMR spectrum, conclusion can be drawn that the other conformation does not exist in solution within the detection limits of the NMR experiment. Upon changing the carbene skeletal framework from imidazolium to benzimidazolium, no significant differences were observed in the bond lengths between the carbene carbon and the palladium center. The degree of elongation of the Pd–Cl bond *trans* to the NHC was also comparable. Furthermore, upon the introduction of bulkier R groups like phenyl, there is a slight increase of about 0.01 Å in the bond lengths between the carbene carbon and the palladium centers compared to the less bulky methyl group. There is also a very slight increase (0.004 Å) in the elongation of the Pd–Cl bond length that is *trans* to the NHC in the case of palladacycle **3** when compared to palladacycle **1**. An increase in the carbene carbon–Pd–Cl (Cl *trans* to the pyridine) bond angle is observed with the increase in the bulkiness of the R group. This can be attributed to the need for the angle enlargement to accommodate the sterically bulkier R group. All of the above observations are summarized in Table 3.

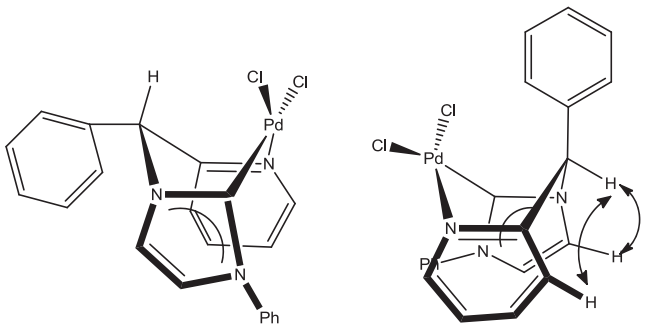

Fig. 6. Two possible conformations of palladacycle **3**.

Resolution of the racemic palladacycles (±)-**2** and (±)-**3** (similar to palladacycle **1**[50]) was performed via screening a range of amino acid salts in methanol. Equimolar amounts of sodium (S_C)-phenylalanate were able to coordinate to (±)-**2**, while sodium (S_C)-prolinate was added to (±)-**3**. The formation of the diastereomeric pair can be confirmed by ^{1}H NMR via the two distinct sets of protons peaks. The diastereomerically pure crystal of (S_C,S_C)-**4** > 99% *de* (according to ^{1}H NMR spectrum) with $[\alpha]_{365} = +202$ ($c = 0.55$, MeOH) formed from (±)-**2** was selectively crystallized by slow diffusion of diethyl ether into an ethanol solution of the diastereomeric mixture. The best diastereomeric ratio was 1:20 with further slow evaporation of the diastereomers mixture in acetonitrile. From the molecular structure (Fig. 7), the *S* absolute configuration of the α-carbon stereocenter can be confirmed using (S_C)-phenylalanate as reference point, as well as based on the anomalous X-ray scattering method with the Flack parameter of 0.001(16). Complex (S_C,S_C)-**4** adopted the *trans*-(*N*,*N*) arrangement, with a boat conformation in the six-membered ring where the phenyl group is occupying the axial position (Table 4). Optically active complex (*S*)-**2** was achieved in 60% yield in the form of yellow powder with $[\alpha]_{436} = -27.8$, ($c = 0.5$, DMSO) via treatment with 1-M HCl (S_C, S_C)-**4** (Scheme 2). Subsequently, the diastereomerically pure complex (S_C,S_C)-**5** formed by reacting (±)-**3** with sodium (S_C)-prolinate was isolated by slow diffusion of diethyl ether into a MeOH solution of the diastereomeric mixture (Fig. 8). It has a diastereomeric purity of >99% *de* with $[\alpha]_{436} = -167$ ($c = 0.5$, MeOH). Similar to complex (S_C,S_C)-**4**, (S_C,S_C)-**5** also adopted the *trans*-(*N*,*N*) arrangement with the six-membered ring in boat conformation (Fig. 9). The selected bond lengths and angles were showed in Table 5.

Following the same method used in Scheme 2, complex (S_C,S_C)-**5** was treated with 1-M HCl to achieve the optically

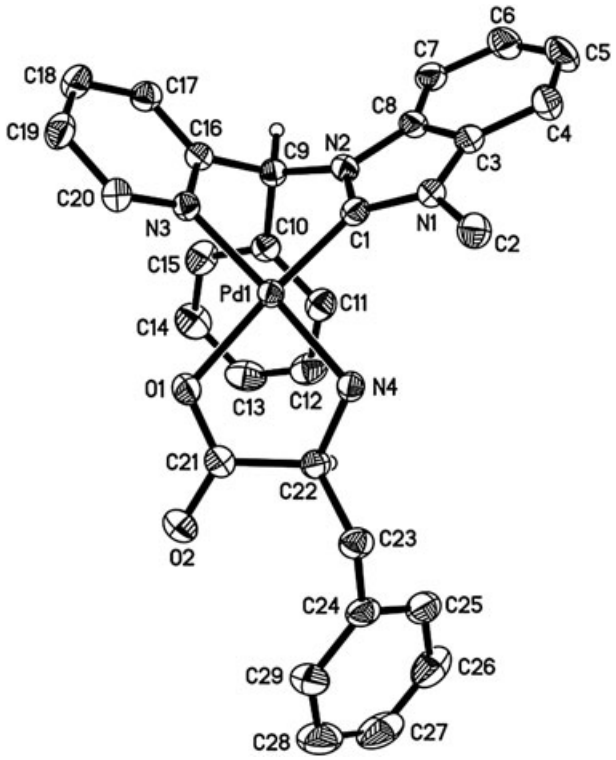

Fig. 7. Molecular structure of (S_C,S_C)-**4**.

TABLE 4. Selected bond lengths (Å) and angles (°) for complex (S_C,S_C)-4

Pd(1)–C(1)	1.950(2)	Pd(1)–N(3)	2.030(16)
Pd(1)–N(4)	2.013(15)	Pd(1)–O(1)	2.047(14)
C(1)–Pd(1)–N(4)	96.73(7)	C(1)–Pd(1)–N(3)	86.75(7)
N(4)–Pd(1)–N(3)	176.34(7)	C(1)–Pd(1)–O(1)	172.62(6)
N(4)–Pd(1)–O(1)	80.77(6)	N(3)–Pd(1)–O(1)	95.91(6)
N(2)–C(1)–Pd(1)	119.08(14)	N(1)–C(1)–Pd(1)	133.26(15)
C(16)–N(3)–Pd(1)	122.70(12)	C(20)–N(3)–Pd(1)	118.22(14)

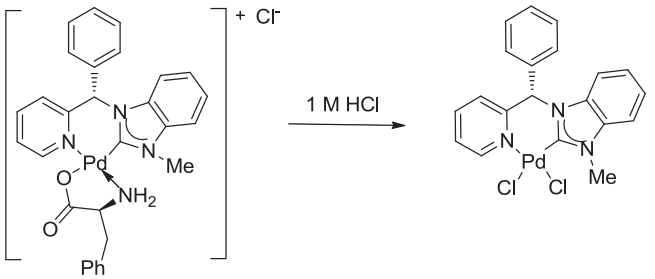

(S_C,S_C)-**4** (S)-**2**

Scheme 2. Removal of chiral auxiliary using 1-M HCl.

pure (S)-**3**. The single crystal X-ray diffraction grade single crystal of palladacycle (S)-**3** (Fig. 10 and Table 6) was obtained from the slow diffusion of diethyl ether into a MeOH/DMSO solution. The absolute configuration at the stereocenter was shown to be *S* and is supported by Flack parameter of −0.005(14). Efforts to crystallize out the complexes (R_C,S_C)-**4**, (R_C,S_C)-**5**, (S)-**2**, (R)-**2**, and (R)-**3** had been unsuccessful to date.

It is well known that one of the chloride ligands in the palladacycles **1–3** can be selectively replaced by stronger incoming ligands such as triphenylphosphine. Therefore, in order to improve the solubility of the complex in organic solvents, one of the chloro ligand on the palladium center had been changed to triphenylphosphine as shown in Scheme 3. The introduction of the bulky triphenylphosphine into the complex is postulated to be able to disrupt the π–π stacking in the crystal lattice and therefore lead to an increase in solubility of the complexes. The resolved palladacycles (R)-**1**, (S)-**1**, (S)-**2**, and (S)-**3** were added to 1 equivalent of triphenylphosphine in dichloromethane and stirred for an

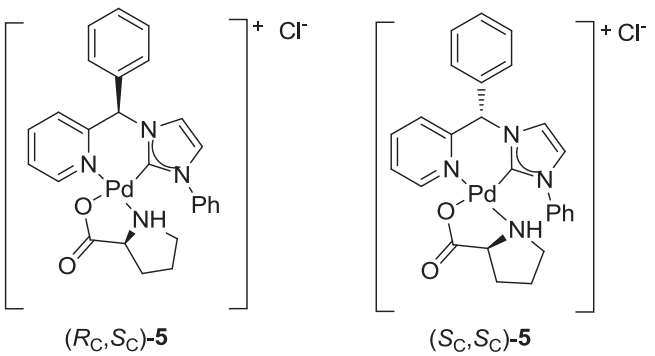

(R_C,S_C)-**5** (S_C,S_C)-**5**

Fig. 8. Diastereomeric mixture of palladacycle **3** with sodium (S_C)-prolinate.

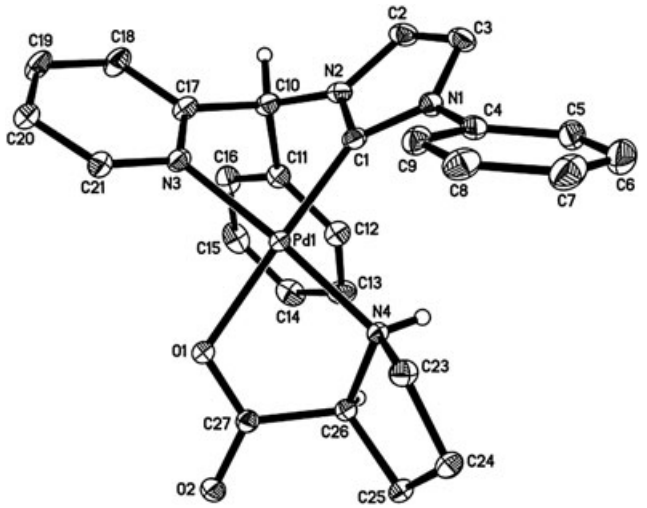

Fig. 9. Molecular structure of complex (S_C,S_C)-**5**.

TABLE 5. Selected bond lengths (Å) and angles (°) for complex (S_C,S_C)-5

Pd(1)–C(1)	1.952(2)	Pd(1)–N(3)	2.022(18)
Pd(1)–N(4)	2.036(17)	Pd(1)–O(1)	2.053(15)
C(1)–Pd(1)–N(4)	97.87(8)	C(1)–Pd(1)–N(3)	85.97(8)
N(4)–Pd(1)–N(3)	172.97(7)	C(1)–Pd(1)–O(1)	171.17(8)
N(4)–Pd(1)–O(1)	81.37(6)	N(3)–Pd(1)–O(1)	93.93(7)
N(2)–C(1)–Pd(1)	118.24(16)	N(1)–C(1)–Pd(1)	136.04(16)
C(17)–N(3)–Pd(1)	121.21(16)	C(21)–N(3)–Pd(1)	119.30(14)

hour to give (R)-**6**, (S)-**6**, (S)-**7**, and (S)-**8**, respectively. The progress of the reaction was monitored by phosphorus-31 (^{31}P) NMR, and all the four chiral palladacycles gave a new single phosphorous peak (summarized in Table 7) indicative of the fact that a single regioisomer was being formed. X-ray diffraction grade crystals are obtained through slow diffusion of diethyl ether into the methanol solution of (R)-**6**,

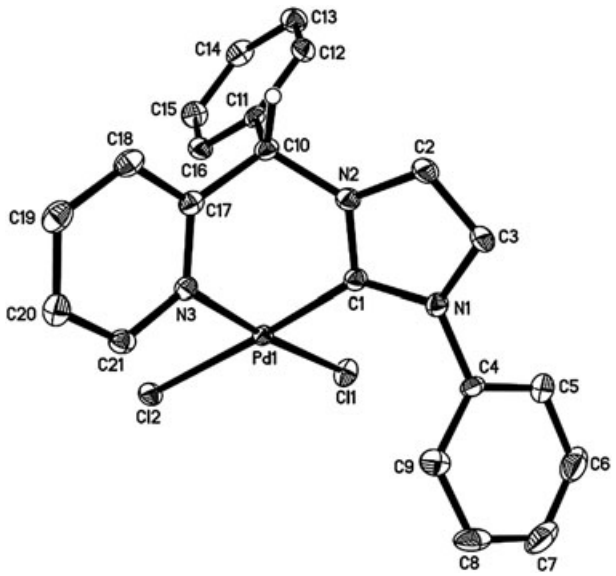

Fig. 10. Molecular structure of (S)-**3**.

TABLE 6. Selected bond lengths (Å) and angles (°) for complex (*S*)-3

Pd(1)–C(1)	1.948(3)	Pd(1)–N(3)	2.047(3)
Pd(1)–Cl(2)	2.376(7)	Pd(1)–Cl(1)	2.301(8)
C(1)–Pd(1)–N(3)	84.8(11)	C(1)–Pd(1)–Cl(1)	91.6(9)
N(3)–Pd(1)–Cl(1)	175.3(8)	C(1)–Pd(1)–Cl(2)	176.2(9)
N(3)–Pd(1)–Cl(2)	91.5(8)	Cl(1)–Pd(1)–Cl(2)	92.0(3)
N(2)–C(1)–Pd(1)	121.5(19)	N(1)–C(1)–Pd(1)	133.5(2)
C(21)–N(3)–Pd(1)	119.5(2)	C(17)–N(1)–Pd(1)	121.5(2)

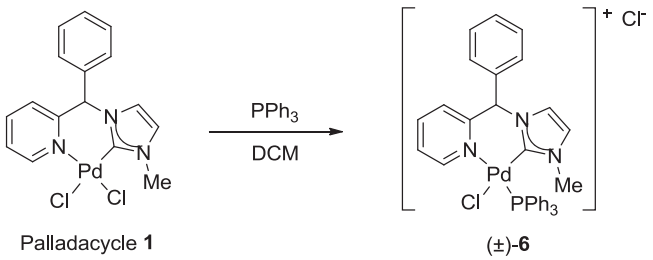

Scheme 3. Replacement of one chloride ion with PPh_3.

(*S*)-**6**, (*S*)-**7**, and (*S*)-**8** shown in Figures 11, 12, and 13, and the selected bond length and angles are tabulated in Tables 8, 9, 10, and 11. Replacement of one of the chloride ions with PPh_3 therefore improved the solubility tremendously in dichloromethane (DCM) with retention of the chiral center. Crystals were obtained easily and ORTEP of (*S*)-**7** is shown in Figure 12 along with significant bond parameters in Table 10.

TABLE 7. Comparison of structures and bond angles (°)

Palladacycle	(*S*)-**6**	(*S*)-7	(*S*)-**8**
^{31}P NMR/ppm	28.31	28.99	26.94
Conformation	Boat	Boat	–
C(1)–Pd(1)–P(1)/°	5.2	4.8	–
Distortion of square planar/°	13.7	6.37	–

Akin to (*S*)-**7**, (*S*)-**8** was prepared as per the procedure illustrated in Scheme 3. A new signal in ^{31}P NMR was observed at 26.94 ppm, and no other resonance signals were seen. Since the phosphorous chemical shift of palladacycle (*S*)-**8** is quite similar to that of palladacycle (*S*)-**7** and (*S*)-**6**, the triphenylphosphine is expected to be coordinated *trans* to the $N_{pyridine}$. Surprisingly, a Pd–N bond cleavage occurred between the $N_{pyridine}$ atom and the palladium center as seen from X-ray diffraction studies (Fig. 13) and as illustrated in Scheme 4. Consequently, complex **9** loses its chirality and became a racemic singly ligated complex. The product was initially isolated as an off-white solid after 1 h and displayed optical activity ($[\alpha]_{436} = -233$, $c = 0.20$, MeOH). However, racemization of the product occurred after 24 h in solution during the crystallization process, and the crystals of racemic complex (±)-**9** were isolated. The product that was stored in the solid form when analyzed for optical activity after 1 week of storage continued to display optical activity. Therefore, racemization of the product only occurred or was accelerated in solution state.

The unexpected bond cleavage may be attributed to the bulkiness of the phenyl substituent on the N of the imidazolium since the $N_{pyridine}$–Pd bond cleavage was not observed in complexes (*S*)-**6** and (*S*)-**7** which have comparatively less bulky methyl group as the substituent on the wingtip N (but initial signs of strain are evident in the bond distances listed in Table 7). Due to the presence of the sterically bulky moeity, the palladium center might not be able to accommodate the triphenylphosphine group while maintaining the bidentate chelating ligand in its coordination sphere. Therefore, the weaker $N_{pyridine}$–Pd bond cleaves in order to create enough space for the incoming triphenylphosphine group. The hemilability of pyridine-functionalized NHC has been observed previously by Lin et al.[51] Upon introduction of triphenylphosphine, an $N_{pyridine}$–Pd cleavage was also observed in their NHC palladium system. The hemilability of this NHC ligand system was further challenged by the use of a weaker and softer coordinating ligand as compared to PPh_3 and triphenylarsine. Scheme 5 shows the possibility of the racemic complex **10** adopting either structure. The X-ray diffraction grade crystal of racemic complex **10** was obtained, and from the X-ray crystallography study, an $N_{pyridine}$–Pd cleavage was observed again even with a weaker

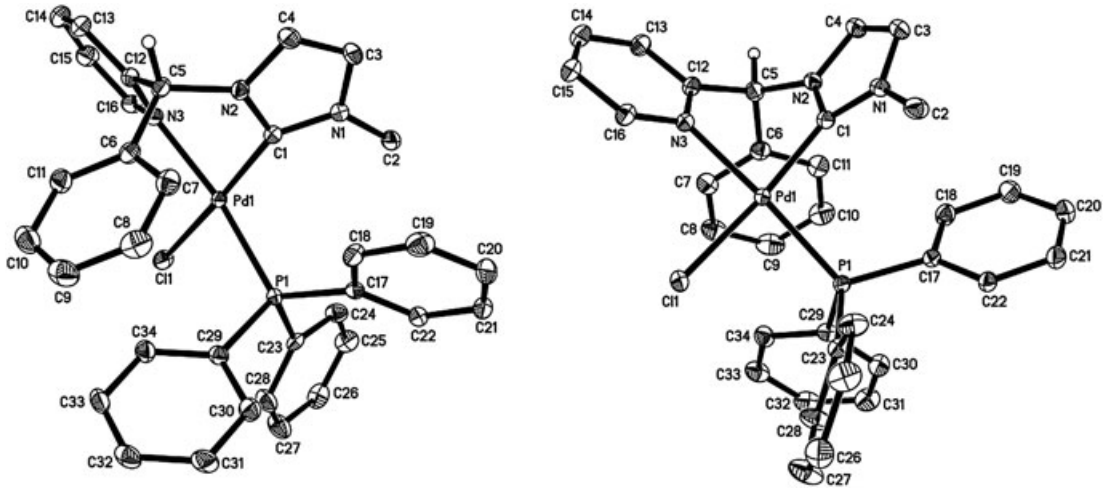

Fig. 11. Molecular structures of (*R*)-**6** and (*S*)-**6**.

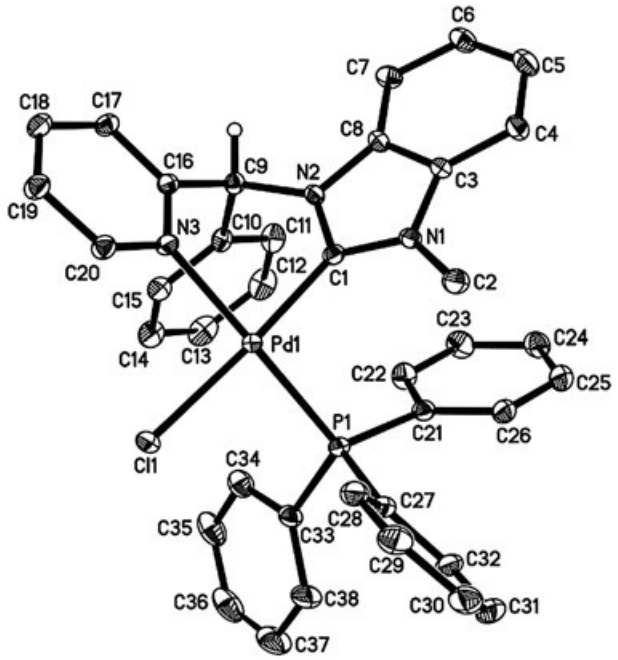

Fig. 12. Molecular structure of (*S*)-**7**.

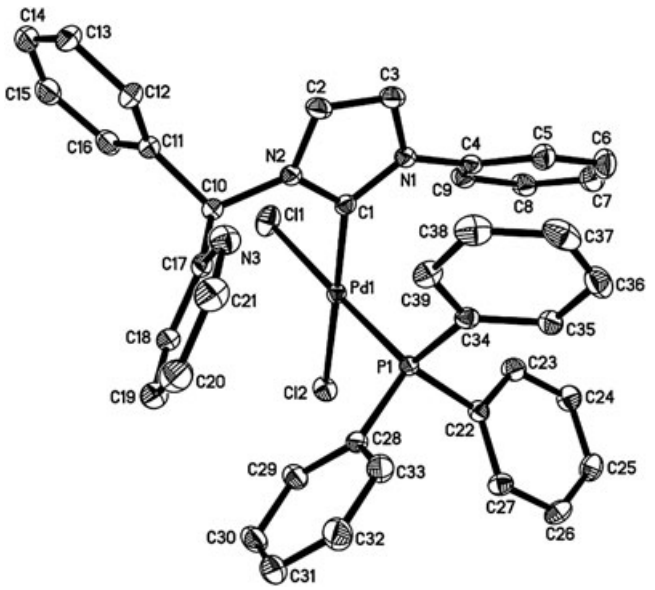

Fig. 13. Molecular structure of racemic complex **9**.

TABLE 8. Selected bond lengths (Å) and angles (°) for complex (*R*)-6

Pd(1)–C(1)	1.975(19)	Pd(1)–N(3)	2.115(16)
Pd(1)–Cl(1)	2.331(4)	Pd(1)–P(1)	2.263(5)
C(1)–Pd(1)–N(3)	83.7(7)	C(1)–Pd(1)–P(1)	97.9(6)
N(3)–Pd(1)–P(1)	168.4(5)	C(1)–Pd(1)–Cl(1)	172.3(6)
N(3)–Pd(1)–Cl(1)	92.5(5)	P(1)–Pd(1)–Cl(1)	87.2(18)
C(23)–P(1)–Pd(1)	113.3(6)	C(17)–P(1)–Pd(1)	116.6(6)
C(29)–P(1)–Pd(1)	109.0(6)	–	–

arsine ligand in comparison to phosphine. Hence, the $N_{pyridine}$–Pd bond in racemic complex **3** exhibits the highest hemilability when compared to complexes **1** and **2**. The molecular

TABLE 9. Selected bond lengths (Å) and angles (°) for complex (*S*)-6

Pd(1)–C(1)	1.977(14)	Pd(1)–N(3)	2.115(12)
Pd(1)–Cl(1)	2.329(3)	Pd(1)–P(1)	2.264(4)
C(1)–Pd(1)–N(3)	83.7(5)	C(1)–Pd(1)–P(1)	97.9(4)
N(3)–Pd(1)–P(1)	168.5(4)	C(1)–Pd(1)–Cl(1)	172.1(5)
N(3)–Pd(1)–Cl(1)	92.4(4)	P(1)–Pd(1)–Cl(1)	87.3(14)
C(17)–P(1)–Pd(1)	116.7(5)	C(29)–P(1)–Pd(1)	109.8(5)
C(23)–P(1)–Pd(1)	113.2(5)	–	–

TABLE 10. Selected bond lengths (Å) and angles (°) for complex (*S*)-7

Pd(1)–C(1)	1.972(1)	Pd(1)–N(3)	2.094(1)
Pd(1)–Cl(1)	2.327(4)	Pd(1)–P(1)	2.274(4)
C(1)–Pd(1)–N(3)	84.12(5)	C(1)–Pd(1)–P(1)	95.78(4)
N(3)–Pd(1)–P(1)	173.55(3)	Cl(1)–Pd(1)–P(1)	88.55(14)
C(1)–Pd(1)–Cl(1)	175.26(4)	N(3)–Pd(1)–Cl(1)	91.80(3)
C(21)–P(1)–Pd(1)	112.2(5)	C(33)–P(1)–Pd(1)	111.9(5)
C(27)–P(1)–Pd(1)	114.3(5)	–	–

TABLE 11. Selected bond lengths (Å) and angles (°) for racemic complex 9

Pd(1)–C(1)	1.979(18)	Pd(1)–P(1)	2.263(5)
Pd(1)–Cl(1)	2.373(5)	Pd(1)–Cl(2)	2.354(5)
C(1)–Pd(1)–Cl(1)	85.5(5)	C(1)–Pd(1)–P(1)	92.7(5)
P(1)–Pd(1)–Cl(2)	89.1(17)	Cl(1)–Pd(1)–Cl(2)	92.4(19)
Pd(1)–P(1)–C(34)	117.16(6)	Pd(1)–P(1)–C(28)	114.49(6)
Pd(1)–P(1)–C(22)	111.15(6)	–	–

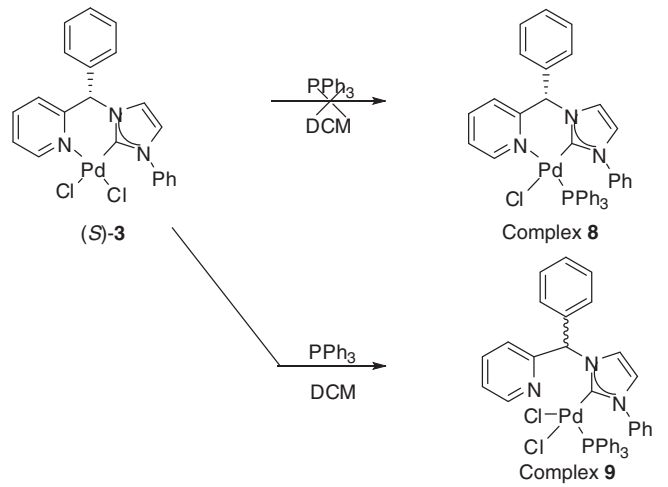

Scheme 4. Removal of one Cl^- ion by PPh_3.

structure of complex **10** is depicted in Figure 14, selected bond length and angles are given in Table 12.

MATERIALS AND METHODS

Reactions involving air-sensitive compounds were performed under a positive pressure of purified nitrogen using standard Schlenk techniques. All the commercially available chemicals and solvents were used without prior drying or purification. $PdCl_2(NCMe)_2$[52] and 1-phenylimidazole[53] were prepared according to literature methods. ^1H and carbon (^{13}C) NMR spectroscopies were performed on a Bruker Avance (Bruker BioSpin AG, Fällanden,Switzerland) 300, 400, and 500 NMR spectrometers

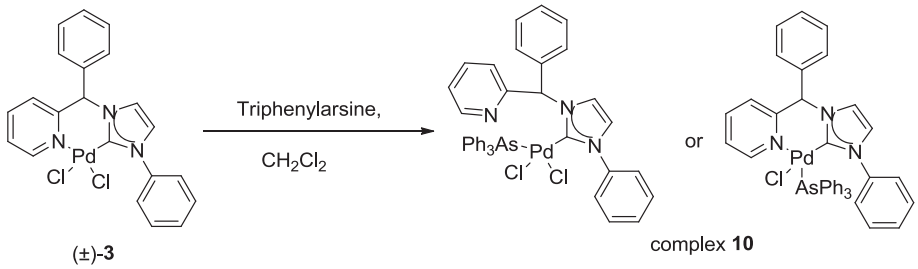

Scheme 5. Analysis of the hemilability of the pyridine group.

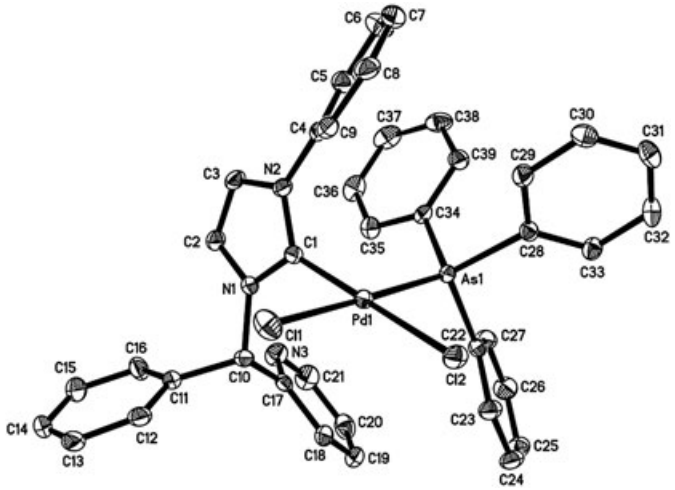

Fig. 14. Molecular structure of racemic complex **10**.

TABLE 12. Selected bond lengths (Å) and angles (°) for racemic complex 10

Pd(1)–C(1)	1.968(2)	Pd(1)–As(1)	2.359(3)
Pd(1)–Cl(1)	2.358(6)	Pd(1)–Cl(2)	2.357(6)
N(1)–C(1)	1.353(3)	N(2)–C(1)	1.357(3)
N(1)–C(2)	1.381(3)	N(2)–C(3)	1.389(3)
N(1)–C(10)	1.482(3)	N(2)–C(4)	1.436(3)
C(1)–Pd(1)–Cl(1)	86.5(6)	C(1)–Pd(1)–As(1)	91.8(6)
As(1)–Pd(1)–Cl(2)	87.9(17)	Cl(1)–Pd(1)–Cl(2)	93.9(2)

(Fällanden, Switzerland). Multiplicities were given as s (singlet), b (broad singlet), d (doublet), t (triplet), q (quartet), dd (doublets of doublet), m (multiplets) etc. The number of protons (*n*) for a given resonance is indicated by nH. Coupling constants are reported as a *J* value in Hz. NMR spectra (^{1}H NMR) are reported as σ in units of parts per million (ppm) downfield from SiMe4 (δ 0.0), relative to the signal of chloroform-d (δ 77.20, triplet) (^{13}C NMR). Phase-sensitive ^{1}H–^{1}H ROESY spectra were obtained with a Bruker AMX-500 spectrometer and were acquired into a 1024 × 512 matrix with a 250-msec spin lock time and a spin lock field strength such that $\gamma B1/2\pi = 5000$ Hz and then transformed into 1024 × 1024 points by using a sine-bell weighting function in both dimensions. Mass spectra were recorded on a Thermo Finnigan MAT 95 XP mass spectrometer (Thermo Fisher Scientific Inc., Waltham, MA, USA) with electron ionization mode and Waters quadrupole time-of-flight Premier mass spectrometer (Waters Corporation, Milford, MA, USA) with electrospray ionization (ESI) mode. Melting points were determined on SRS-Optimelt MPA-100 apparatus and were uncorrected. Optical rotations were measured on the specified solution in 0.1-dm cell at 25 °C with a PerkinElmer model 341 polarimeter (Waltham, MA, USA). Single crystal X-ray diffraction data were collected on a Bruker X8 CCD diffractometer with Mo Kα radiation (graphite monochromator). SADABS absorption corrections were applied. All non-hydrogen atoms were refined anisotropically, while the hydrogen atoms were introduced at calculated positions and refined riding on their carrier atoms. The absolute configurations of the chiral complexes were determined unambiguously by using the Flack parameter. CCDC 841566, 841567, and 875261–875266 contain the supplementary crystallographic data for complexes **2**, **3**, and (*Sc*, *Sc*)-**4**, (*Sc*-*Sc*)-**5**, (*S*)-**3**, (*R*)-**6**, (*S*)-**6**, (*S*)-**7**, **9**, and **10**, respectively. These data can be obtained free of charge from The Cambridge Crystallographic Data Center *via* www.ccdc.cam.ac.uk/data_request/cif.

EXPERIMENTAL

1-Methyl-3-(phenyl(pyridin-2-yl)methyl)-1*H*-benzo[*d*]imidazol-3-ium chloride, [10]. Solid 1-methylbenzimidazole (3.24 g, 24.5 mmol) was added to a stirring solution of compound **5** (5.00 g, 24.5 mmol) in 50 ml of CH_3CN. The reaction mixture was heated at refluxing temperature for 48 h. The reaction mixture was reduced in vacuo, and the resulting oil was stirred in diethyl ether. The diethyl ether layer was decanted away to give an off-white solid, 5.3 g, 64%. ^{1}H NMR (400 MHz, $CDCl_3$): δ = 4.30 (s, 3H, CH3), 7.31–7.34 (m, 1H, aromatic protons), 7.39–7.44 (m, 5H, aromatic protons), 7.46–7.48 (m, 1H, aromatic proton), 7.56–7.61 (m, 2H, aromatic protons), 7.65–7.67 (m, 2H, aromatic protons), 7.76–7.78 (m, 1H, aromatic proton), 7.84 (t, 1H, $J_{H,H}$ = 3.9 Hz, aromatic proton), 8.56 (d, 1H, $J_{H,H}$ = 4.2 Hz, aromatic proton), 11.33 (s, 1H, imidazolium proton) ppm. ^{13}C NMR (100 MHz, $CDCl_3$): δ = 33.99 (N–CH3), 67.23 (N–C–Ph), 112.56, 116.16, 124.27, 124.77, 126.95, 127.07, 128.98, 129.61, 129.72, 131.57, 132.51, 134.87, 138.15, 144.27, 149.97, 154.73, 155.93. HRMS (ESI) *m/z*: $[M - Cl]^+$ calcd for C16H16N3 300.1501, found 300.1503.

1-Phenyl-3-(phenyl(pyridin-2-yl)methyl)-1*H*-imidazol-3-ium chloride, [11]. Liquid 1-phenylimidazole (3.24 g, 24.5 mmol) was added to a stirring solution of compound **5** (5.00 g, 24.5 mmol) in 50 ml of CH_3CN. The reaction mixture was heated at refluxing temperature for 48 h. The reaction mixture was reduced in vacuo, and the resulting oil was stirred in diethyl ether. The diethyl ether layer was decanted away to give an off-white solid, 5.3 g, 64%. ^{1}H NMR (400 MHz, $CDCl_3$): δ = 6.65 (s, 1H, aromatic proton), 7.28–7.31 (m, 1H, aromatic proton), 7.35–7.37 (m, 3H, aromatic protons), 7.42–7.52 (m, 3H, aromatic proton), 7.56–7.58 (m, 2H, aromatic protons), 7.68–7.76 (m, 5H, aromatic protons), 7.92 (s, 1H, aromatic proton), 8.17 (s, 1H, aromatic proton), 8.59 (d, 1H, $J_{H,H}$ = 4.7 Hz, aromatic proton), 11.18 (s, 1H, imidazolium proton) ppm. ^{13}C NMR (100 MHz, $CDCl_3$): δ = 65.97 (N–C–Ph), 116.26, 119.64, 121.78, 123.52, 123.90, 124.87, 129.20, 129.35, 129.51, 130.26, 130.64, 134.58, 136.19, 136.46, 137.80, 149.47, 150.10, 155.06 ppm. HRMS (ESI) *m/z*: $[M - Cl]^+$ calcd for C21H18N3 312.1501, found 312.1501.

Racemic palladacycle [2]. To a solution of compound **10** (4.50 g, 13.4 mmol) in 30 ml of CH_2Cl_2, Ag_2O (1.70 g, 7.3 mmol) was added in the dark. The reaction mixture was stirred at room temperature for 12 h and was filtered through celite. A $PdCl_2(NCMe)_2$ suspension (3.48 g, 13.4 mmol in 100 ml of CH_3CN) was added to the filtrate in the dark. The reaction mixture was then stirred overnight at room temperature and was filtered through a short plug of celite the next day. The filtrate was reduced in vacuo to approximately 50 ml, and diethyl ether (200 ml)

was added which resulted in the precipitation of an orange-yellow solid 4.01 g, 63%. mp = 330.0–330.5 °C (dec). ^{1}H NMR (400 MHz, DMSO): δ = 4.20 (s, 3H, CH3), 7.36–7.39 (m, 2H, aromatic protons), 7.41–7.46 (m, 3H, aromatic proton), 7.52 (quintet, 2H, $J_{H,H}$ = 7.0 Hz, aromatic proton), 7.65 (t, 1H, $J_{H,H}$ = 6.3 Hz, aromatic proton), 7.80 (d, 1H, $J_{H,H}$ = 7.3 Hz, aromatic proton), 7.85 (s, 1H, aromatic proton), 8.15–8.18 (m, 2H, aromatic proton), 8.23 (t, 1H, $J_{H,H}$ = 7.5 Hz, aromatic proton), 9.14 (s, 1H, aromatic proton) ppm. ^{13}C NMR (100 MHz, DMSO): δ = 35.26 (N–CH3), 63.36 (N–C–Ph), 110.83, 111.98, 124.51, 125.31, 126.41, 126.98, 128.44, 128.94, 132.90, 134.18, 138.06, 140.62, 154.40, 155.19, 163.76 ppm. HRMS (ESI) *m/z*: $[M - H]^+$ calcd for C20H16Cl2N3Pd 475.9727, found 475.974.

Racemic palladacycle [3]. To a solution of compound **11** (4.50 g, 13.4 mmol) in 30 ml of CH_2Cl_2, Ag_2O (1.70 g, 7.3 mmol) was added in the dark. The reaction mixture was stirred at room temperature for 12 h and was filtered through celite. A $PdCl_2(NCMe)_2$ suspension (3.48 g, 13.4 mmol in 100 ml of CH_3CN) was added to the filtrate in the dark. The reaction mixture was then stirred overnight at room temperature and was filtered through a short plug of celite the next day. The filtrate was reduced in vacuo to approximately 50 ml, and diethyl ether (200 ml) was added which resulted in the precipitation of an orange-yellow solid 4.01 g, 63%. mp = 294.8–296.5 °C (dec). ^{1}H NMR (400 MHz, DMSO): δ = 7.36 (s, 1H, aromatic proton), 7.39–7.45 (m, 4H, aromatic protons), 7.47–7.58 (m, 4H, aromatic protons), 7.69 (t, 1H, $J_{H,H}$ = 6.7 Hz, aromatic proton), 7.83–7.86 (m, 3H, aromatic proton), 8.05–8.08 (m, 2H, aromatic proton), 8.24 (t, 1H, $J_{H,H}$ = 7.9 Hz, aromatic proton), 9.23 (s, 1H, aromatic proton) ppm. ^{13}C NMR (100 MHz, DMSO): δ = 67.16 (N–C–Ph), 123.15, 123.87, 124.91, 125.21, 127.15, 128.07, 128.45, 128.65, 128.84, 137.81, 139.18, 140.47, 154.17, 155.16 ppm. HRMS (ESI) *m/z*: $[M - H]^+$ calcd for C21H16Cl2N3Pd 487.9727, found 487.9719.

Optical resolution of racemic complexes (−)-[2] and (+)-[2]. Sodium (S_C)-phenylalanate (0.98 g, 5.2 mmol) was added to a suspension of the racemic complex (±)-**2** (2.50 g, 5.2 mmol) in 100 ml of MeOH. The reaction mixture was stirred for 1 h and was concentrated in vacuo. The residue was redissolved in ethanol, and diethyl ether was allowed to diffuse into the solution slowly. Diastereomer (S_C,S_C)-**4** which crystallized out as off-white crystals the next day was isolated and washed with ethanol. Complex (R_C, S_C)-**4** enriched mother liquor was concentrated to dryness and redissolved in acetonitrile. Slow evaporation of the acetonitrile solution allowed the remaining diastereomer (S_C,S_C)-**4** to crystallize out.

Diastereomer (S_C,S_C)-**4** 0.9 g, 60%, $[\alpha]_{365}$ = +202 (*c* = 0.55, MeOH), mp = 215.9–216.5 °C (dec). ^{1}H NMR (400 MHz, DMSO): δ = 2.82–2.87 (m, 1H), 3.13 (dd, 1H, $J_{H,H}$ = 14.0 Hz, $J_{H,H}$ = 1.7), 3.22–3.24 (m, 1H), 3.95 (s, 3H, CH_3), 5.73–5.77 (m, 2H), 7.23 (t, 1H, $J_{H,H}$ = 6.9 Hz, aromatic proton), 7.29–7.36 (m, 4H, aromatic protons), 7.39–7.40 (m, 3H, aromatic protons), 7.49–7.52 (m, 4H, aromatic protons), 7.73–7.77 (m, 1H, aromatic protons), 7.82–7.86 (m, 1H, aromatic protons), 8.01 (s, 1H, aromatic proton), 8.13–8.17 (m, 1H, aromatic proton), 8.32–8.39 (m, 2H, aromatic proton), 8.72 (d, 1H, $J_{H,H}$ = 5.4 Hz, aromatic proton) ppm. ^{13}C NMR (100 MHz, DMSO): δ = 34.00, 61.46, 62.48, 111.12, 111.82, 124.50, 126.08, 126.40, 126.67, 128.43, 128.53, 128.86, 129.26, 132.76, 134.01, 137.78, 137.91, 141.73, 152.22, 154.85, 164.25, 177.30 ppm. HRMS (ESI) *m/z*: $[M - Cl]^+$ calcd for $C_{29}H_{27}N_4O_2^{106}Pd$ 569.1169, found 569.1183.

Chiral complex (*S*)-[2]. To a suspension of complex (S_C,S_C)-**4** (0.50 g, 0.83 mmol) in 1 ml of MeOH, 1-M HCl (aq) (8.3 ml, 8.3 mmol) was added. The reaction mixture was stirred vigorously for approximately 1 h and was concentrated down to give a pale yellow solid. The solid was washed three times with copious amount of MeOH to give a pale yellow solid 0.26 g, 66%, $[\alpha]_{365}$ = +405 (*c* = 0.21, DMSO).

Optical resolution of racemic complexes (−)-[3] and (+)-[3]. Sodium (S_C)-prolinate (0.70 g, 5.1 mmol) was added to a suspension of the racemic complex (±)-**3** (2.50 g, 5.1 mmol) in 100 ml of MeOH. The reaction mixture was stirred for 1 h and was concentrated in vacuo. The residue was redissolved in MeOH, and diethyl ether was allowed to diffuse into the solution slowly. Diastereomer (S_C,S_C)-**5** which crystallized out as off-white crystals the next day was isolated and washed with CH_2Cl_2. The complex (R_C,S_C)-**5** enriched mother liquor was concentrated to dryness and redissolved in ethanol.

Diastereomer (S_C,S_C)-**5** 1.8 g, 62%, $[\alpha]_{436}$ = −167 (*c* = 0.5, MeOH), mp = 222.4–223.5 °C (dec). ^{1}H NMR (400 MHz, DMSO): δ = 0.98–1.04 (m, 1H), 1.15–1.26 (m, 1H), 1.40–1.52 (m, 1H), 1.56–1.66 (m, 1H), 1.86–2.01 (m, 1H), 2.29–2.38 (m, 1H), 3.22 (dd, 1H, $J_{H,H}$ = 8.6 Hz, $J_{H,H}$ = 2.9 Hz), 7.23 (d, 2H, $J_{H,H}$ = 7.0 Hz, aromatic protons), 7.34 (s, 1H, aromatic proton), 7.43–7.51 (m, 3H, aromatic protons), 7.62–7.70 (m, 3H, aromatic proton), 7.74–7.79 (m, 2H, aromatic proton), 7.86–7.87 (m, 2H, aromatic proton), 8.10 (d, 1H, $J_{H,H}$ = 2.0 Hz, aromatic protons), 8.13 (d, 1H, $J_{H,H}$ = 7.4 Hz, aromatic protons), 8.32 (td, 1H, $J_{H,H}$ = 7.7 Hz, $J_{H,H}$ = 1.5 Hz, aromatic protons), 8.88 (d, 1H, $J_{H,H}$ = 4.8 Hz, aromatic proton) ppm. ^{13}C NMR (100 MHz, DMSO): δ = 23.74, 29.15, 68.19, 69.07, 125.23, 125.63, 127.27, 127.37, 128.28, 130.13, 130.37, 131.46, 139.74, 140.56, 142.87, 154.42, 155.95, 182.17 ppm. HRMS (ESI) *m/z*: $[M - Cl]^+$ calcd for $C_{26}H_{25}N_4O_2^{106}Pd$ 531.1012, found 531.1014.

Chiral complex (*S*)-[3]. To a suspension of complex (S_C,S_C)-**5** (0.50 g, 0.88 mmol) in 1 ml of MeOH, 1-M HCl (aq) (8.8 ml, 8.8 mmol) was added. The reaction mixture was stirred vigorously for approximately 1 h and was concentrated down to give a pale yellow solid. The solid was washed three times with copious amount of MeOH to give a pale yellow solid 0.28 g, 65%, $[\alpha]_{436}$ = −27.8 (*c* = 0.20, DMSO).

Chiral complex (*S*)-[7]. To a suspension of complex (*S*)-**2** (0.1 g, 0.21 mmol) in 10 ml of CH_2Cl_2, triphenylphosphine (0.055 g, 0.21 g) was added. The solution was stirred for 1 h. After 1 h, the clear solution was concentrated to dryness. The product was purified through precipitation in CH_2Cl_2 and diethyl ether to give an off-white solid 0.15, 97%, $[\alpha]_{436}$ = −37 (*c* = 0.57, MeOH), mp = 209.0–210.9 °C (dec). ^{1}H NMR (400 MHz, MeOD): δ = 3.15 (s, 3H, CH_3), 6.51 (s, 1H), 6.97 (t, 2H, $J_{H,H}$ = 7.8 Hz, aromatic proton), 7.11–7.25 (m, 11H, aromatic protons), 7.36–7.42 (m, 6H, aromatic protons), 7.51 (t, 2H, aromatic protons), 7.09–7.33 (m, 11H, aromatic protons), 7.56–7.59 (m, 1H, $J_{H,H}$ = 7.1 Hz, aromatic proton), 7.65 (t, 2H, $J_{H,H}$ = 6.0 Hz, aromatic proton), 7.72 (s, 1H, aromatic proton), 8.04 (d, 1H, $J_{H,H}$ = 7.10 Hz, aromatic proton), 8.14 (t, 1H, $J_{H,H}$ = 8.2 Hz, aromatic proton), 8.18 (d, 1H, $J_{H,H}$ = 7.8 Hz, aromatic proton), 9.23–9.24 (m, 1H, aromatic proton) ppm. ^{13}C NMR (100 MHz, MeOD): δ = 36.17, 65.95,112.06, 112.79, 126.79, 126.68, 127.01, 127.80, 127.82, 128.73, 129.69, 129.80, 130.47, 130.64, 132.90, 135.14, 135.81, 140. 09, 142.48, 151.25, 155.02, 155.11, 174.15 ppm. ^{31}P{1H} (161 MHz, MeOD): δ = 28.99 ppm. HRMS (ESI) *m/z*: $[M - Cl]^+$ calcd for $C_{38}H_{32}ClN_3PPd$ 704.1061, found 704.1055.

Complex [9]. To a suspension of complex (*S*)-**3** (0.1 g, 0.20 mmol) in 10 ml of CH_2Cl_2, triphenylphosphine (0.053 g, 0.20 mmol) was added. The solution was stirred for 1 h. After 1 h, the clear solution was concentrated to dryness. The product was purified through precipitation in DCM and diethyl ether to give an off-white solid 0.148 g, 98%. ^{1}H NMR (400 MHz, MeOD): δ = 6.33 (s, 1H), 7.03 (t, 2H, $J_{H,H}$ = 7.8 Hz, aromatic proton), 7.17–7.27 (m, 13H, aromatic proton), 7.32–7.35 (m, 4H, aromatic protons), 7.39 (s, 2H, aromatic protons), 7.41–7.47 (m, 5H, aromatic protons), 7.82 (t, 1H, $J_{H,H}$ = 6.6 Hz, aromatic proton), 8.04 (d, 1H, $J_{H,H}$ = 7.6 Hz, aromatic proton), 8.13 (s, 1H, aromatic proton), 8.29 (t, 1H, $J_{H,H}$ = 7.7 Hz, aromatic proton), 9.45–9.46 (m, 1H, aromatic proton). ^{13}C NMR (100 MHz, MeOD): δ = 70.17, 125.12, 125.29, 126.25, 127.08. 127.96, 128.58, 129.41, 130.34, 130.40, 130.70, 130.96, 132.46, 136.14, 138.93, 139.36, 142.46, 155.00. 155.23, 161.88 ppm. ^{31}P{1H} (161 MHz, MeOD): δ = 26.94 ppm. HRMS (ESI) *m/z*: $[M - Cl]^+$ calcd for $C_{39}H_{32}N_3ClP^{108}Pd$ 716.1016, found 716.1068.

Complex (±)-[10]. To a suspension of complex (±)-**3** (0.1 g, 0.20 mmol) in 10 ml of DCM, triphenylarsine (0.063 g, 0.20 mmol) was added. The solution was stirred for 1 h. After 1 h, the clear solution was concentrated to dryness. The product was purified through precipitation in DCM and diethyl ether to give an off-white solid 0.16 g, 98%. ^{1}H NMR (400 MHz, MeOD): δ = 6.63 (s, 1H), 6.94–6,97 (m, 2H, aromatic protons), 7.19 (t, 2H, $J_{H,H}$ = 8.0 Hz, aromatic protons), 6#?>7.25–7.37 (m, 14H, aromatic protons), 7.40 (s, 1H, aromatic proton), 7.49 (t, 3H, $J_{H,H}$ = 8.0 Hz, aromatic proton), 7.54 (d, 1H, $J_{H,H}$ = 4.0 Hz, aromatic protons), 7.63–7.67 (m,

1H, aromatic proton), 7.71–7.75 (m, 2H, aromatic protons), 7.84–7.87 (m, 1H, aromatic proton), 8.08 (d, 1H, $J_{H,H}$ = 8.0 Hz, aromatic proton), 8.16 (d, 1H, $J_{H,H}$ = 2.0 Hz, aromatic proton), 8.33 (dt, 1H, $J_{H,H}$ = 7.7 Hz, $J_{H,H}$ = 1.5 Hz, aromatic proton), 9.49 (d, 1H, $J_{H,H}$ = 4.7 Hz aromatic proton) ppm. ^{13}C NMR (100 MHz, MeOD): δ = 70.17, 116.82, 124.87, 124.96, 126.12, 126.26, 127.25, 128.10, 128.56, 129.78, 129.94, 130.13, 130.35, 130.50, 130.95, 131.03, 131.97, 132.46, 134.09, 134.71, 139.01, 139.62, 142.61, 142.61, 154.90, 155.32, 164.02 ppm. HRMS (ESI) *m/z*: $[MH - Cl]^+$ calcd for $C_{39}H_{33}N_3ClAs^{108}Pd$ 761.0618, found 761.0627.

CONCLUSION

We have successfully synthesized and comprehensively characterized two new pyridine-functionalized NHC palladacycles and analyzed their conformational rigidity both in solid state and in solution via single crystal X-ray diffraction studies and 2D ^{1}H–^{1}H NMR analysis. It was seen that upon replacing one of the chloride ions with PPh_3 in a regioselective manner, the solubility of these complexes improved tremendously with the retention of the chiral center and also led to easier crystallization. Interestingly, cleavage of the $N_{pyridine}$–Pd bond that occurred in complex **9** demonstrated the hemilability of the pyridine-functionalized NHC palladacycle and is indicative of a limitation imposed by steric bulkiness of the wingtip group. Based on the information obtained from the conformational rigidity analysis, we are currently exploring the synthesis of other versions of these catalysts with a view of exploring their potential in various asymmetric catalysis scenarios.

ACKNOWLEDGMENT

We thank Prof. Leung Pak-Hing for fruitful discussions.

LITERATURE CITED

1. Fischer EO, Maasbol A. On the existence of tungsten carbonyl carbene complex. Angew Chem Int Ed 1964;3:580–581.
2. Schrock RR. Alkylcarbene compex of tantalum by intramolecular alpha-hydrogen abstraction. J Am Chem Soc 1974;96:6796–6796.
3. Arduengo AJ, Harlow RL, Kline M. A stable crystalline carbine. J Am Chem Soc 1991;113:361–363.
4. Fröhlich N, Pidun U, Stahl M, Frenking G. Carbenes as pure ligand donors: theoretical study of beryllium-carbene complexes. Organometallics 1997;16:442–448.
5. Jacobsen H, Correa A, Costabile C, Cavallo L. π-acidity and π-basicity of N-heterocyclic ligands. A computational assessment. J Organomet Chem 2006;691;4350–4358.
6. Díez-González S. Nolan SP. Stereoelectronic parameters associated with N-heterocyclic carbene (NHC) ligands: a quest for understanding. Coord Chem Rev 2007;251:874–883.
7. Fantasia S, Petersen JL, Jacobsen H, Cavallo L, Nolan SP. Electronic properties of N-heterocyclic carbene (NHC) ligands: synthetic, structural and spectroscopic studies of (NHC)platinum(II) complexes. Organometallics 2007;26:5880–5889.
8. Khramov DM, Lynch VM, Bielawski CW. N-heterocyclic-transition metal complexes: spectroscopic and crystallographic analysis of π-back bonding interactions. Organometallics 2007;26:6042–6049.
9. Hahn FE, Jahnke MC. Heterocyclic carbenes: synthesis and coordination chemistry. Angew Chem Int Ed 2008;47:3122–3172.
10. Scholl M, Ding S, Lee CW, Grubbs RH. Synthesis and activity of a new generation of ruthenium-based olefin metathesis catalysis coordinated with 1,3-dimesityl-4,5-dihydroimidazol-2-ylidene ligands. Org Lett 1999;1:953–956.
11. Herrmann WA, Elison M, Fischer J, Köcher C, Artus GRJ. Metal complexes of N-heterocyclic carbenes—a new structural principle for catalyst in homogenous catalysis. Angew Chem Int Ed 1995;34:2371–2374.
12. Herrman WA, Reisinger C-P, Spiegler M. Chelating N-heterocyclic carbene ligands in palladium-catalyzed Heck-typed reactions. J Organomet Chem 1998;557:93–96.
13. Caddick S, Cloke FGN, Clentsmith GKB, Hitchcock PB, McKerrecher D, Titcomb LR, Wiliams MRV. An improved synthesis of bis(1,3-di-*N*-*tert*-butylimidazol-2-ylidene)palladium(0) and its use in C–C and C–N coupling reactions. J Organomet Chem 2001;617:635–639.
14. Huang J, Nolan SP. Efficient cross-coupling of aryl chlorides with aryl grinard reagents (Kumada reactions) mediated by a palladium/imidazolium chloride system. J Am Chem Soc 1999;121:9889–9890.
15. Frisch AC, Rataboul F, Zapf A, Beller M. First Kumada reaction of alkyl chloride using N-heterocyclic carbene/palladium catalyst system. J Organomet Chem 2003;687:403–409.
16. Zhou JR, Fu GC. Palladium catalyzed Neigishi cross-coupling reactions of unactivated alkyl iodide, bromides, chlorides and tosylates. J Am Chem Soc 2003;125:12527–12530.
17. Hadei N, Kantchev EAB, O'Brien CJ, Organ MG. The first Neigishi cross-coupling reaction of two alkyl centres utilizing a Pd-N-heterocyclic carbene (NHC) catalyst. Org Lett 2005;7:3805–3807.
18. Organ MG, Arola S, Dubovyk I, Hadei N, Kantchev EAB, O'Brien CJ, Valente C. A user-friendly, all-purpose Pd-NHC precatalyst for the Negishi reaction: a step towards a universal cross-coupling catalyst. Chem Eur J 2006;12:4749–4755.
19. Herrmann WA, Böhm VPW, Gstöttmayr GWK, Grosche M, Resinger C-P, Weskamp T. Synthesis, structure and catalytic application of palladium(II) complexes bearing N-heterocyclic carbenes and phosphines. J Organomet Chem 2001;617:616–628.
20. Grasa GA, Nolan SP. Palladium/imidazolium salt catalyzed coupling of aryl halides with hypervalent organostannates. Org Lett 2001;3:119–122.
21. J.K. Huang, G. Grasa, S.P. Nolan. General and efficient catalytic amination of aryl chlorides using a palladium/bulky nucleophilic carbene system. Org Lett 1991;1:1307–1309.
22. Goossen LJ, Paetzold J, Briel O, Rivas-Nass A, Karch R, Kayser B. Buchwald–Hartwig aminations of aryl chlorides: a practical protocol based on commercially available Pd(0)-NHC catalysts. Synlett 2005;2:275–278.
23. Marion N, Navarro O, Mei JG, Stevens ED, Scott NM, Nolan SP. Modified (NHC)Pd(allyl)Cl complexes for room temperature Suzuki–Miyuara and Buchwald–Hartwig reactions. J Am Chem Soc 2006;128:4101–4111.
24. Marion N, Ecarnot EC, Navarro O, Amoroso D, Bell A, Nolan SP. (IPr)Pd(acac)Cl: an easily synthesized, efficient and versatile precatalyst for C–N and C–C bond formation. J Org Chem 2006;71:3816–3821.
25. Broggi J, Clavier H, Nolan SP. N-heterocyclic carbenes (NHCs) containing N–C–palladacycle complexes: synthesis and reactivity in aryl amination reactions. Organometallics 2008;27:5525–5531.
26. Lee SW, Hartwig JF. Improved catalyst for the palladium-catalyzed synthesis of oxindoles by amid α-arylation. Rate acceleration, use of aryl chloride substrates, and a new carbene ligand for asymmetric transformations. J Org Chem 2001;66:3402–3415.
27. Kündig EP, Seidel TM, Jia YX, Bernardinelli G. Bulky chiral carbene ligands and their application in the palladium-catalyzed asymmetric intramolecular α-arylation of amides. Angew Chem Int Ed 2007;46:8484–8487.
28. Zhang T, Shi M. Chiral bidentate bis(N-heterocyclic carbene)-based palladium complexes bearing carboxylate ligands: highly effective catalyst for the enantioselective conjugate addition of arylboronic acids to cyclic enones. Chem Eur J 2008;14:3759–3764.
29. Xu Q, Zhang R, Zhang T, Shi M. Asymmetric 1,4-addition of arylboronic acids to 2,3-dihydro-4-pyridones catalyzed by axially chiral NHC–Pd(II) complexes. J Org Chem 2010;75:3935–3937.
30. Ma GN, Zhang T, Shi M. Catalytic enantioselective arylation of *N*-tosylarylamines with arylboronic acids using C_2-symsetric cationic N-heterocyclic carbene Pd^{2+} diaquo complexes. Org Lett 2009;11:875–878.
31. Kuhl O. The chemistry of functionalized N-heterocyclic carbenes. Chem Soc Rev 2007;36:592–607.
32. Ludovic GB, Douthwaite RE, Hodgson R, Houghton J, Kariuki BM, Simonovic S. Synthesis, structure and reactivity of palladium(II) complexes of chiral N-heterocyclic carbene-imine and -amine hybrid ligands. Dalton Trans 2004;21:3528–3535.
33. Ludovic GB, Douthwaite RE, Kariuki BM. Synthesis of new chiral N-heterocyclic carbene-imine ligands and their application to an asymmetric allylic alkylation reaction. Organometallics 2003;22:4187–4189.
34. Chianese AR, Bremer PT, Wong C, Reynes RJ. Rigid, sterically diverse N-heterocyclic carbene-pyridine chelates: synthesis, mild palladation and palladium catalyzed allylic substitution. Organometallics 2009;28:5244–5252.

35. Tulloch AAD, Danopoulos AA, Tooze RP, Cafferkey SM, Kleinhenz S, Hursthouse MB. Pyridine functionalized N-heterocyclic carbene complexes of palladium. Chem Commun 2000;14:1247–1248.
36. Tulloch AAD, Danopoulos AA, Kleinhenz S, Light ME, Hursthouse MB, Eastham G. Structural diversity in pyridine-N-functionalized carbene copper (I) complexes. Organometallics 2001;20:2027–2031.
37. Tulloch AAD, Winston S, Danopoulos AA, Eastham G, Hursthouse MB. Functionalized and chelate heterocyclic carbene complexes of palladium; synthesis and structural studies. Dal Trans 2003;4:699–708.
38. Winston S, Stylianides N, Tulloch AAD, Wright JA, Danopoulos AA. Picoline and pyridine functionalized chelate N-heterocyclic carbene complexes of nickel: synthesis and structural studies. Poly 2004;23:2813–2820.
39. Wang CY, Liu YH, Peng SM, Lin ST. Rhodium(I) complexes containing a bulky pyridinyl N-heterocyclic carbene ligand: preparation and reactivity. J Organometallic Chem 2006;691:4012–4020.
40. Chang Y, Xu HJ, Sun JF, Li YZ, Chen XT, Xue ZL. Synthesis, structure and catalytic activities of ruthenium(II) carbonyl chloride complexes containing pyridine-functionalized N-heterocyclic carbene. Dal Trans 2009;35:7132–7140.
41. Danopoulos AA, Tsoureas N, Macgregor SA, Smith C. Phosphine- and pyridine-functionalized N-heterocyclic carbene methyl and allyl complexes of palladium. Unexpected regiospecificity of the protonation reaction of the dimethyl complexes. Organometallics 2007;26:253–263.
42. McGuinness DS, Gibson VC, Wass DF, Steed JW. Bis(carbene)pyridine complexes of Cr(III): exceptionally active catalyst for the oligomerization of ethylene. J Am Chem Soc 2003;125:12716–12717.
43. Danopoulos AA, Tsoureas N, Wright JA, Light ME. N-heterocyclic pincer dicarbene complexes of iron(II): C-2 and C-5 metalated carbenes on the same metal center. Organometallics 2004;23:166–168.
44. Danopoulos AA, Wright JA, Motherwell MB. Molecular N_2 complexes of iron stabilized by N-heterocyclic 'pincer' dicarbene ligands. Chem Commun 2005;6:784–786.
45. Simons RS, Custer P, Tessier CA, Youngs WJ. Formation of N-heterocyclic complexes of rhodium and palladium from a pincer silver(I) carbene complex. Organometallics 2003;22:1979–1982.
46. Wong CY, Lai LM, Pat PK, Chung LH. Osmium complexes containing N-heterocyclic carbene-based C–N–C–pincer ligands. Organometallics 2010;29:2533–2539.
47. Gründemann S, Albrecht M, Loch JA, Faller JW, Crabtree RH. Tridentate carbene CCC and CNC pincer palladium(II) complexes: structure, fluxionality and catalytic activity. Organometallics 2001;20:5485–5488.
48. Loch JA, Albrecht M, Peris E, Mata J, Faller JW, Crabtree RH. Palladium complexes with tridentate pincer bis-carbene ligands as efficient catalyst for C–C coupling. Organometallics 2002;21:700–706.
49. Hahn FE, Jahnke MC, Gomez-Benitez V, Morales-Morales P, Pape T. Synthesis and catalytic activity of pincer-type bis(benzimidazolin-2-ylidene) palladium complexes. Organometallics 2005;24:6458–6463.
50. Chiang MY, Li YX, Krishnan D, Sumod P, Ng KH, Leung PH. Synthesis and characterization of a novel chiral bidentate pyridine N-heterocyclic carbene-based palladacycle. Eur J Inorg Chem 2010;9:1413–1418.
51. Chen JCC, Lin IJB. Palladium complexes containing a hemilabile pyridylcarbene ligand. Organometallics 2000;19:5113–5121.
52. Mathews CJ, Smith PJ, Welton T. N-donor complexes of palladium as catalysts for Suzuki cross-coupling reactions in ionic liquids. J Mol Cat A: Chem. 2004;214:27–32.
53. Rout L, Jammi S, Punniyamurthy T. Novel CuO nanoparticle catalyzed C–N cross-coupling of amines with iodobenzene. Org Lett 2007;9:3397–3399.